

# First observation of $^{109}\text{Te} \beta^+$ and electron capture decay to levels of $^{109}\text{Sb}$

J. J. Ressler,<sup>1,2,3</sup> W. B. Walters,<sup>1</sup> C. N. Davids,<sup>2</sup> D. J. Dean,<sup>4</sup> A. Heinz,<sup>2</sup> M. Hjorth-Jensen,<sup>5</sup> D. Seweryniak,<sup>2</sup> and J. Shergur<sup>1</sup>

<sup>1</sup>Department of Chemistry, University of Maryland, College Park, Maryland 20742

<sup>2</sup>Physics Division, Argonne National Laboratory, Argonne, Illinois 60439

<sup>3</sup>A. W. Wright Nuclear Structure Laboratory, Yale University, New Haven, Connecticut 06520

<sup>4</sup>Physics Division, Oak Ridge National Laboratory, P.O. Box 2008, Oak Ridge, Tennessee 37831-6373

<sup>5</sup>Department of Physics, University of Oslo, Oslo, Norway

(Received 31 March 2002; published 6 August 2002)

Low-spin levels in  $^{109}\text{Sb}$  populated by  $^{109}\text{Te}$  beta decay are reported for the first time. Seven new levels are proposed, two below 1 MeV excitation energy. Spins and parities of  $(1/2^+)$  and  $(3/2^+, 5/2^+)$  are suggested for the low energy levels by comparison to beta feeding intensities and systematics. These results are compared with new calculated levels for  $^{109}\text{Sb}$ .

DOI: 10.1103/PhysRevC.66.024308

PACS number(s): 23.40.-s, 23.20.Lv, 21.60.Cs, 27.60.+j

## I. INTRODUCTION

Nuclear structure studies near the doubly magic  $N$  and  $Z = 50$  shell gap have long been of interest both theoretically and experimentally. Above the shell gap, the  $d_{5/2}$ ,  $g_{7/2}$ , and  $h_{11/2}$  spherical single quasiparticle orbitals are easily observed in the odd-mass nuclei. The odd-mass Sb isotopes are of particular interest as there is only a single proton beyond the  $Z = 50$  closed shell. Energy states below the neutron pairing energy ( $\sim 2$  MeV) arise from single proton excitations and the proton coupling to collective states in the even-even Sn core.

Collective structures have been recently identified in the light Sn-Sb-Te-I region, often coexisting with the spherical single particle orbitals. In the odd-proton nuclei, the collective bands are thought to arise from particle-hole excitations across the  $Z = 50$  gap. A coupling between a hole in the  $g_{9/2}$  orbital with a two-quasiparticle structure or a single-quasiparticle coupling to  $2p-2h$  excitations of the Sn core are attributed to the collective bands observed in  $Z = 51$  Sb. Hence, a wealth of medium-spin structures associated with the  $h_{11/2}$  particle and  $g_{9/2}$  hole are available for the light Sb isotopes [1,2].

In contrast, there have been few studies of the low-spin structure beyond proton transfer reactions into  $^{113}\text{Sb}$  and heavier isotopes [3]. From the transfer reactions studies, the first  $5/2^+$  and  $7/2^+$  states of the light odd- $A$  Sb isotopes are shown to have very high single-particle character, 75–80% [4]. The first  $1/2^+$  and  $3/2^+$  levels, however, have very weak single-particle character. These states are assumed to have configurations involving a weak coupling of the  $5/2_1^+$  and  $7/2_1^+$  states with the first  $2^+$  level of the appropriate Sn core.

Low-spin states in  $^{109}\text{Sb}$  are expected to lie 700–1000 keV above the ground state, similar to what has been observed in the heavier  $^{115-119}\text{Sb}$  isotopes. These states have been observed in a study of  $^{109}\text{Sb}$  structure following  $^{109}\text{Te}$  beta decay. The beta decay of  $^{109}\text{Te}$  is reported here for the first time.

## II. EXPERIMENT

The experiment was performed at the ATLAS facility of Argonne National Laboratory. An accelerated beam of  $^{58}\text{Ni}$

ions was used to bombard a stationary  $^{54}\text{Fe}$  target of  $615 \mu\text{g}/\text{cm}^2$ . A beam energy of 260 MeV was used for 10 h, and then shifted to 230 MeV for the remaining 24 h of the experiment.

Reaction recoils were mass/charge separated through the fragment mass analyzer (FMA), which was tuned to select recoils of  $A = 109$  and  $Q = 25$ . Mechanical slits were used on either side of the FMA focal plane to limit the intensity of other  $A/Q \neq 109/25$  recoils. Relative intensities for the  $A/Q$  separated recoils are shown in Fig. 1 with and without the use of the slits.

Nuclei with  $A = 108$  and  $Q = 25$  are produced with a high

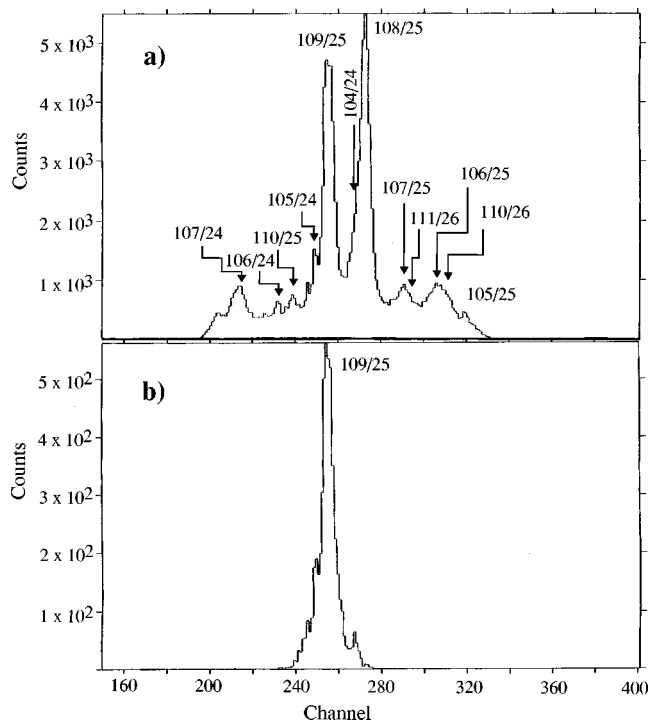


FIG. 1. Mass over charge separation through the Argonne fragment mass analyzer. Spectra are obtained from horizontal distribution in a proportional counter located at the focal plane of the mass spectrometer. In (a), the mechanical slits are fully retracted. In (b), the slits are narrowed to optimize observation of  $A/Q = 109/25$ .

cross section, and form a tail under the  $A/Q=109/25$  peak exiting the FMA. While the intensity of these recoils was significantly reduced by the use of the slits, they are still observed. Recoils of  $A=105$  and  $A=104$  with  $Q=24$  are also observed despite the slits. Recoils with  $A=105$  ( $A/Q=4.375$ ) form a small peak near  $A=109$  ( $A/Q=4.360$ ). To maximize the intensity of the  $A=109$  recoils, the left slit was not used to remove the  $A=105$  recoils. Recoils with  $A=104$  and  $Q=24$  ( $A/Q=4.333$ ) form a distribution under  $A=108$  ( $A/Q=4.320$ ). Similar to the  $A=108$  peak, the tail of the  $A=104$  peak extends under the chosen  $A=109$  peak.

Separated recoils were then implanted onto the tape of a moving tape collector. The tape was advanced at 9-s intervals to a shielded counting station consisting of three high-purity (HP) Ge detectors. A low-energy photon spectrometer and a 70% Ge detector were placed opposite to one another on either side and as close as possible to the tape transport pipe. An 80% Ge detector was hung from above at a distance of  $\sim 10$  cm from the tape. Beta absorbers of 1-cm-thick aluminum were placed in front of the 70% and 80% HP Ge detectors.

Gamma singles, gamma-gamma coincidences, and gamma-time data were collected and analyzed.

### III. RESULTS

The  $^{109}\text{Te}$  beta-decay parent has been previously identified in both alpha-decay and delayed proton emission [5] studies. A decay half-life of 4.6(3) s [6] has been reported. As the  $^{109}\text{Te}$  decay half-life is shorter than many neighboring nuclei, the gamma-time data was used to separate short-lived decays by subtracting the energy spectrum collected during the second half of the counting cycle from the spectrum collected during the first half. The resultant spectrum, shown in Fig. 2, displays short-lived transitions as peaks while longer-lived transitions subtract to approximately zero. Granddaughter transitions that grow in during the counting period appear as dips. Strong peaks at 402-, 752-, and 832 keV are easily identified in the subtracted spectrum.

The time-dependent decay of the 402-, 752-, and 832-keV peaks correlate to half-lives in the range of 4–5 s for all three transitions, suggesting they arise from the 4.6-s  $^{109}\text{Te}$  decay. However, interferences with gamma decays from neighboring nuclides introduced uncertainties in the peak areas of both the 402- and 832-keV transitions. The 402-keV decay intensity is affected by the very strong 397-keV transitions following the decay of  $^{108}\text{Sn}$  and 401-keV transitions following the decay of  $^{104}\text{Sn}$ . The 832-keV transition is known to belong to  $^{109}\text{Sb}$ , assigned as the decay from the first excited state to ground in high-spin studies [2,7]. This transition is concurrent with an 831-keV transition in  $^{109}\text{Sn}$ , an 832-keV transition in  $^{105}\text{Cd}$ , and an 834-keV transition in  $^{104}\text{Cd}$ .

Due to the uncertainty of the 402- and 832-keV intensities, only the decay of the 752-keV intensity was used to determine a half-life for  $^{109}\text{Te}$ . A 4.6(3)-s half-life, in excellent agreement with the previously reported value, was calculated by a weighted least squares fit to the 752-keV intensity, shown in Fig. 3.

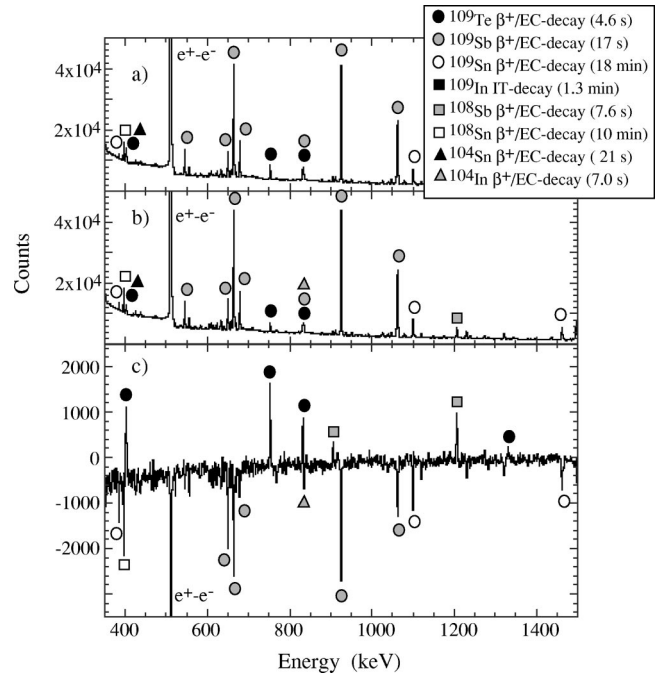


FIG. 2. Time-subtracted spectrum showing  $^{109}\text{Sb}$  transitions. The gamma energy spectrum collected 4.0–8.9 s following a tape move (b) was subtracted from the spectrum collected within the first 3.9 s (a). Short-lived transitions are present only in the earlier time gate and appear as peaks in the subtracted spectrum shown in (c). Long-lived transitions subtract to zero. Granddaughter transitions predominate in the latter time gate and appear as dips in the subtracted spectrum. The spectrum has been attenuated such that the full intensity of the 511-keV annihilation radiation is not shown.

From the  $\gamma$ - $\gamma$  coincident data, additional  $^{109}\text{Sb}$  transitions following  $^{109}\text{Te}$   $\beta^+$ /EC decay were sought. Only weak coincidences with the three strongest transitions (402, 752, and 832 keV) were observed; none of the three strongest transitions were coincident with another. The observed coincidences are shown in Figs. 4–6. The top spectrum in each figure is the gated energy while directly below (in gray) is the background. The energy gate is shown with a +25-keV offset for clarity purposes. The background gate was subtracted from the energy gate to produce the difference spec-

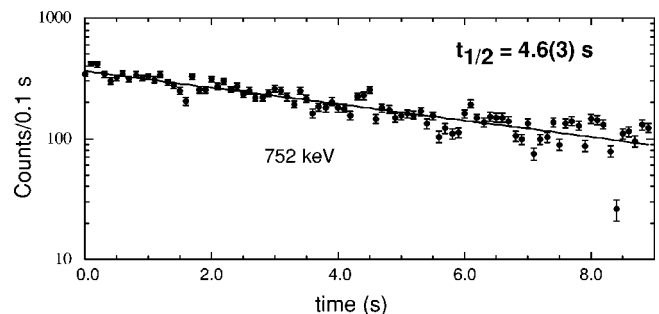


FIG. 3.  $\beta^+$ /EC-half-life determination for  $^{109}\text{Te}$ . The intensity of the 752-keV transition is shown as a function of time following a tape movement. A weighted least squares fit to these data determines a 4.6(3) s for the  $\beta^+$ /EC-decay half-life of  $^{109}\text{Te}$ .

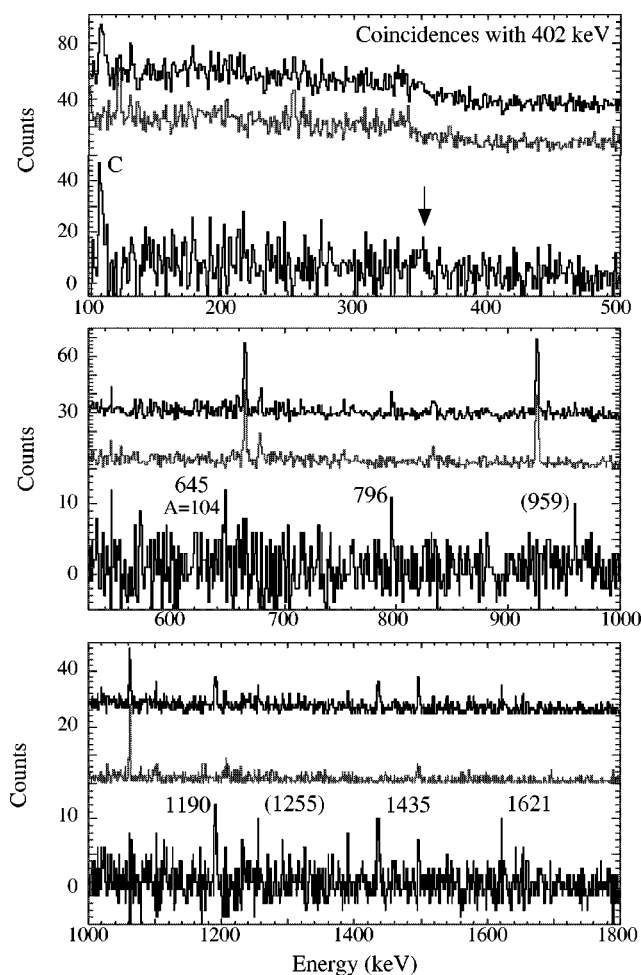


FIG. 4. Coincidences with the 402-keV transition of  $^{109}\text{Sb}$ . Energy gated (top, black), background (gray), and subtracted spectra (bottom, black) are shown as a function of energy. The energy gated spectrum is offset by +25 counts for clarity. A possible peak may be at 350 keV, corresponding to a decay from the 752-keV level. The broad peak at 109 keV is due to Compton scatter of the 511-keV annihilation gamma. The peak at 645 keV is the  $(2^+)_2$  to  $(3^+)_1$  states in  $^{104}\text{In}$ . This transition is in coincidence with a 401-keV  $(1^+)_1$  to  $(2^+)_2$  transition following  $^{104}\text{Sn } \beta^+/\text{EC}$  decay.

tra, bottom. Energy and background gates are displayed to show true peaks in the subtracted spectra.

The strength of the 402-, 752-, and 832-keV transitions and lack of mutual coincidences suggest excited levels at these energies above longer-lived states. A  $7/2^+$  level at 832 keV above the ground state in  $^{109}\text{Sb}$  has been observed previously [2,7]. Levels at 402- and 752-keV have not been reported, and may be new levels above the ground state or a long-lived isomer. As long-lived isomeric states have not been observed in the light Sb isotopes, the 402- and 752-keV transitions are tentatively assigned as decays from new levels above the 17-s ground state of  $^{109}\text{Sb}$ . The new levels are assumed to be low spin due to the nature of this experiment and their omission in the high-spin study.

The in-beam work suggested a  $9/2^+$  level at 1101 keV decaying both to the ground and the  $7/2^+$  excited state at

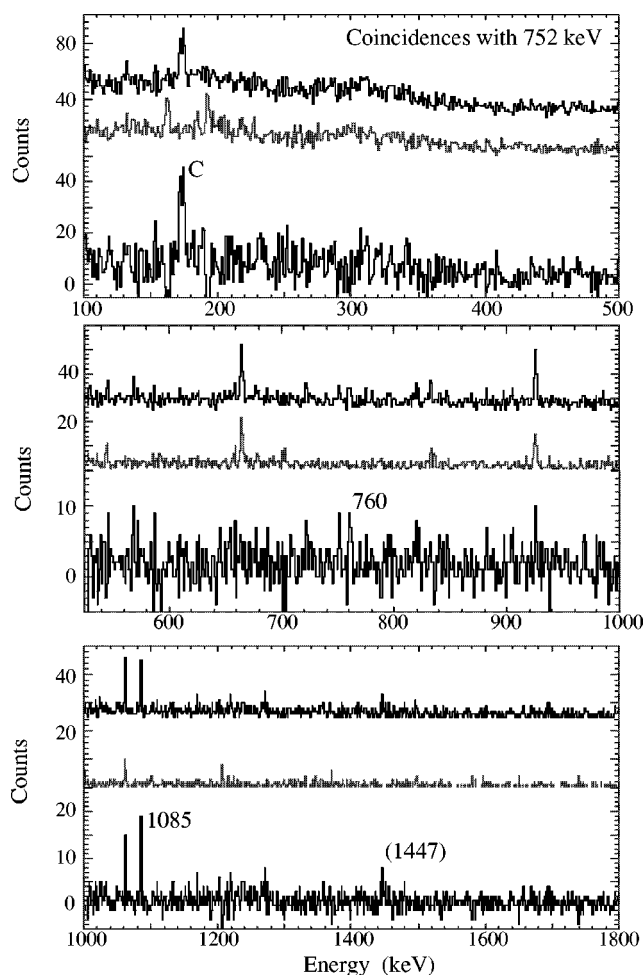


FIG. 5. Coincidences with the 752-keV transition of  $^{109}\text{Sb}$ . See caption for Fig. 4. The broad peak at 173 keV is due to Compton scatter of the 925-keV gamma following  $^{109}\text{Sb}$  beta decay. The strong peak at 1062 keV is thought to arise from poor background subtraction. An intense 1062-keV transition is well known in  $^{109}\text{Sn}$ .

832 keV. The decay energy between the  $9/2^+$  and  $7/2^+$  states is 269 keV, and is weakly observed in the 832-keV coincidence spectrum. This confirms population of  $^{109}\text{Sb}$ .

A transition of 1331 keV with a 4.2(9)-s half-life is observed in the time-subtracted spectrum and may be tentatively assigned to  $^{109}\text{Sb}$ . No coincidences with this transition were observed. A weak 1101-keV transition was also seen, further confirming a population of the  $9/2^+$  state at 1101 keV. The 1101-keV coincidence spectra was heavily contaminated by the intense 1099-keV transition following  $^{109}\text{Sn}$  beta decay. Coincidences from the low-energy and high-energy shoulders of the 1100-keV peak were compared. Transitions of 918, 964, and 1101 keV were observed in the higher-energy coincident spectrum only, and are not assigned to  $^{109}\text{In}$ . These may be transitions feeding the 1101-keV level in  $^{109}\text{Sb}$ . A 918-keV transition directly feeding the 1101-keV level would arise from a new level at 2019 keV. In the 832-keV coincident spectrum, a weak 1186-keV transition is observed. This transition may be a decay from the same level as described above. However, neither the 918- nor the 1186-keV transitions are observed above background levels in the

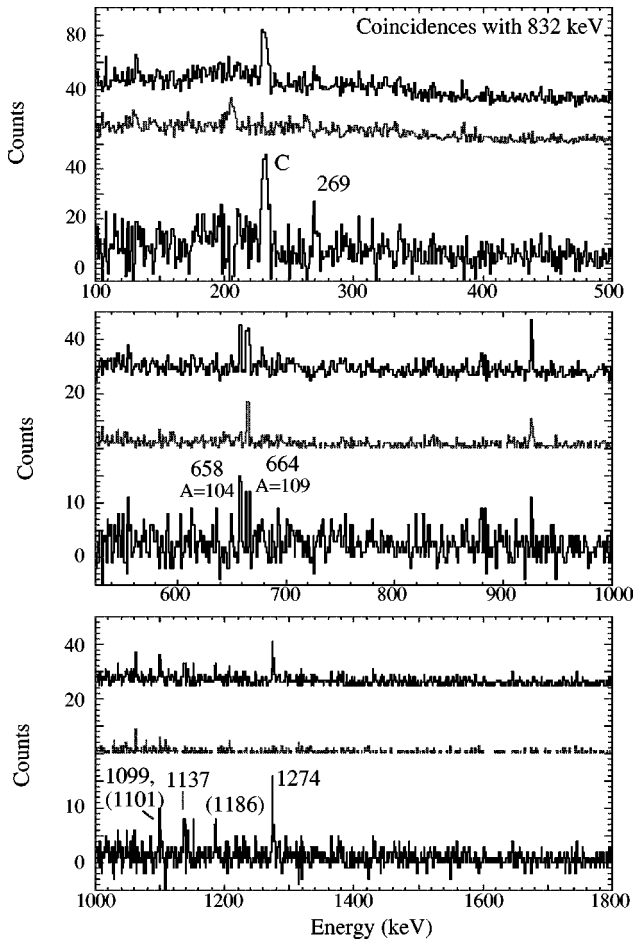


FIG. 6. Coincidences with the 832-keV transition of  $^{109}\text{Sb}$ . See caption for Fig. 4. The broad peak at 230 keV is due to Compton scatter of the 1062-keV gamma following  $^{109}\text{Sb}$  beta decay. The peak at 658 keV is the  $2^+ - 0^+$  transition of  $^{104}\text{Cd}$  which is due to an energy gate overlap with the 834-keV  $4^+ - 2^+$  transition of this nuclide. The transition of 664 is due to an energy overlap with a 831-keV transition in  $^{109}\text{Sn}$ . The presence of the 1099-keV transition may be due to an energy overlap with a transition of 829 keV in  $^{109}\text{In}$ .

time-subtracted data. Due to the uncertainties in the 1101-keV coincidence spectrum, the weakness of the 1186-keV transition, and the lack of the 918 and 1186 transitions in the time data, this new level is only tentative.

Possible transitions from new levels suggested by the coincidences in Figs. 4–6 were sought in the time-subtracted data shown in Fig. 2. Weak evidence for 1592- and 1969-keV transitions can be observed, supporting levels at these energies. Transitions of 1190 and 1137 keV are also weakly observed, further supporting the proposed new levels. The 1274-keV transition is unfortunately concurrent with a 1273-keV transition in  $^{108}\text{Sb}$  decay. The remaining transitions may be too weak to be seen, or the coincidences above may arise from Compton scatter events. From the coincidence and time data, an energy level scheme for  $^{109}\text{Sb}$  following beta decay of  $^{109}\text{Te}$  is proposed in Fig. 7 and summarized in Table I.

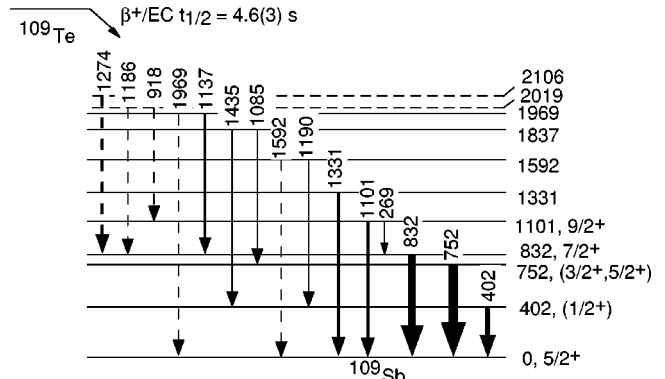


FIG. 7. Tentative level scheme for  $^{109}\text{Sb}$  following  $^{109}\text{Te}$  decay. Level energies and transitions are shown in units of keV. Uncertain levels and transitions are shown with dashed lines. Only the 832- and 1101-keV excited levels have been observed previously (Refs. [2,7]). The relative intensity of the gamma transition is shown by the arrow width.

#### IV. SHELL MODEL CALCULATIONS

Experimental energy levels for  $^{109}\text{Sb}$  may be compared to shell model calculations in the region. The theoretical scheme is to obtain an effective two-body interaction starting from the free nucleon-nucleon interaction  $V$  that is appropriate for descriptions of nuclear physics at low and intermediate energies. Thus, the charge-dependent version of the Bonn potential models was adopted as a starting point [8]. This and other modern nucleon-nucleon interactions typically have a strongly repulsive core that may be renormalized by building a reaction  $G$  matrix. In diagrammatic language the  $G$  matrix represents the sum over all ladder diagrams. The  $G$  matrix is incomplete in the sense that it only sums to all orders the particle-particle ladder diagrams. The long-range effects represented by core-polarization terms must also be included. The long-range effects are incorporated by renormalizing the  $G$ -matrix elements by the  $\hat{Q}$ -box method. Nonfolded, irreducible, and valence linked diagrams make up the  $\hat{Q}$  box. All nonfolded diagrams to third order in  $G$  [9] were included. An effective interaction  $\tilde{H}$  was then calculated in terms of the  $\hat{Q}$  box using the folded-diagram expansion method; see Ref. [9] for further details.

The effective two-particle interaction in large-scale shell model calculations is used. The shell model problem is an eigenvalue problem, requiring the solution to  $\tilde{H}|\Psi_k\rangle = E_k|\Psi_k\rangle$ , with  $k=1, \dots, K$ . The Lanczos algorithm was employed to find the lowest (and highest) eigenvalues and eigenvectors (up to  $K=10-50$ , typically). The basic algorithm adopted here was first proposed in Ref. [10].

The shell model space consisted of the orbitals  $2s_{1/2}$ ,  $1d_{5/2}$ ,  $1d_{3/2}$ ,  $0g_{7/2}$ , and  $0h_{11/2}$  for both protons and neutrons. The single-particle energies were (in units of MeV), for protons, 3.45, 0.0, 3.55, 0.2, and 3.0, and for the neutrons, 2.55, 0.0, 2.45, 0.2 and 3.0, respectively. We note that as the number of active valence particles grows in a given single-particle space, the size of the calculation grows quite quickly. Table II shows some examples.

A  $(5/2)^+$  ground state for the odd Sb systems was consis-

TABLE I. Gamma intensities in  $^{109}\text{Sb}$  following  $^{109}\text{Te}$  beta decay. Energy errors are  $\pm 0.4$  keV. Intensities are relative to the 752-keV transition.

Level energy (keV)	To level (keV)	$\gamma$ -ray energy (keV)	Relative intensity
0			
402	0	402.0	50(3)
752	0	752.3	100
832	0	831.6	79(5)
1101	832	268.6	$\leq 10$
	0	1101.0	30(4)
1330	0	1330.8	32(4)
1592	402	1189.8	11(4)
	0	(1592)	$\leq 10$
1837	752	1085.0	$\leq 10$
	402	1435.4	15(9)
1969	832	1136.9	21(5)
	0	(1969)	$\leq 10$
(2019)	832	(1186)	10(3)
	1101	(918)	$\leq 10$
2106	832	1274.1	27(11)
(1619)	0	1619.5	10(1)
(2045)	0	2045.5	7(1)
Unplaced transitions in coincidence with (keV)			
402		796, 959, (1255), 1621	
752		760, (1447)	
832		(1101)	
1101		964, 1101	

tently obtained. This is contrary to what is observed for the tin isotopes. For  $^{109}\text{Sn}$ , the ground state changes to  $(7/2)^+$ . The ground state is essentially dominated by a proton in the  $\pi d_{5/2}$  orbit, with occupations 0.78, 0.85, 0.86, and 0.87, respectively, as we move from  $^{103}\text{Sb}$  to  $^{109}\text{Sb}$ . Neutrons are essentially distributed over the  $\nu d_{5/2}$  and  $\nu g_{7/2}$  orbits, with  $\nu d_{5/2}$  the dominating orbit. If the neutron occupations for the ground states of these isotopes are compared with the corresponding occupation probabilities of the ground states of the even  $^{102}\text{Sn}$ ,  $^{104}\text{Sn}$ ,  $^{106}\text{Sn}$ , and  $^{108}\text{Sn}$  isotopes, similar values are found. The ground state of the antimony isotopes may therefore be modeled as a system consisting of an even tin ground state with  $J=0^+$  coupled to a proton quasiparticle with angular momentum  $J=(5/2)^+$ .

TABLE II. Number of basis states for selected Sb isotopes.

System	Dimension	System	Dimension
$^{103}\text{Sb}$	$7.8 \times 10^2$	$^{105}\text{Sb}$	$4.2 \times 10^4$
$^{107}\text{Sb}$	$9.1 \times 10^5$	$^{109}\text{Sb}$	$9.6 \times 10^7$
$^{112}\text{Sb}$	$1.1 \times 10^8$	$^{116}\text{Sb}$	$1.9 \times 10^9$

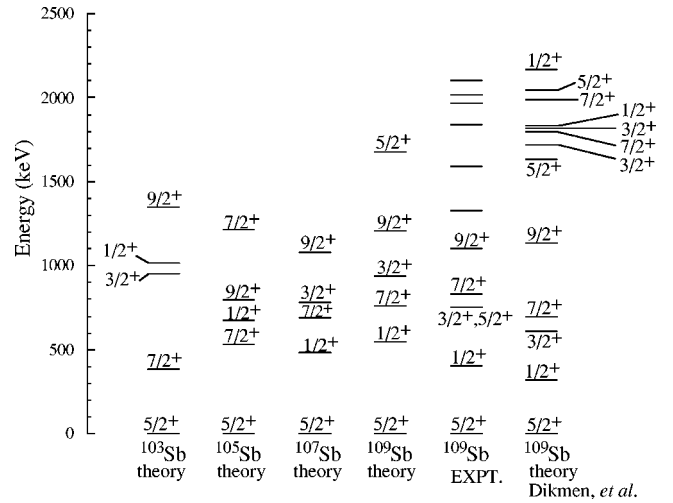


FIG. 8. Experimental and calculated energy levels for  $^{109}\text{Sb}$ . Shell model calculations for  $^{103-109}\text{Sb}$  are shown on the left (see text for details). Experimental levels for  $^{109}\text{Sb}$  are adopted from this work. A comparison to shell model calculations by Dikmen *et al.* (Refs. [11,12]) is also shown on the far right.

One interesting feature of the experiment and the theory is the relative position of the first excited  $(7/2)^+$  and first excited  $(1/2)^+$  states. They invert order as one adds neutrons to  $^{103}\text{Sb}$ . The proton  $d_{5/2}$  occupation of the first excited  $(1/2)^+$  is 0.58, 0.65, 0.69, and 0.71 as the mass increases from  $^{103}\text{Sb}$  to  $^{109}\text{Sb}$ . The neutron  $d_{5/2}$  and  $g_{7/2}$  are the levels that primarily change occupation for this state. The first excited  $(7/2)^+$  is essentially a proton in the  $g_{7/2}$  orbital, with occupation probabilities of 0.77, 0.85, 0.81, and 0.83 for  $^{103}\text{Sb}$ ,  $^{105}\text{Sb}$ ,  $^{107}\text{Sb}$ , and  $^{109}\text{Sb}$ , respectively. The neutron occupation probabilities are in turn rather similar to those of the corresponding even Sn isotopes, indicating again that this state as well can be modeled upon the ground state of the even Sn isotopes coupled to a proton quasiparticle, but now with angular momentum  $J=(7/2)^+$ . This has important consequences since it allows extrapolations of the proton quasiparticle states to  $^{101}\text{Sb}$  and thereby infers the proton single-particle energies for  $^{100}\text{Sn}$ . The extrapolation of the shell model data yield a spacing for  $\pi d_{5/2} - \pi g_{7/2} = 0.24$  MeV for  $^{101}\text{Sb}$ .

Results of these shell model calculations for the light Sb isotopes are shown in Fig. 8 with experimental energy levels of  $^{109}\text{Sb}$ . Also shown are  $^{109}\text{Sb}$  shell model calculation levels by Dikmen *et al.* [11,12]. Dikmen's levels were proposed independently of this experiment.

## V. SPIN AND PARITY ASSIGNMENTS

As there is little experimental data available for medium- and low-spin states of very light Sb and Te nuclides, interpretations for the observed structure is difficult. Beta decays for the Te isotopes have been observed as low as  $^{113}\text{Te}$ .

The amount of beta feeding from  $^{109}\text{Te}$  to each level in  $^{109}\text{Sb}$  can be estimated by the difference of gamma intensities entering and exiting each state. The most intensely beta fed state is suggested to be the new level at 752 keV, as this state is only weakly fed from the proposed level at 1837 keV,

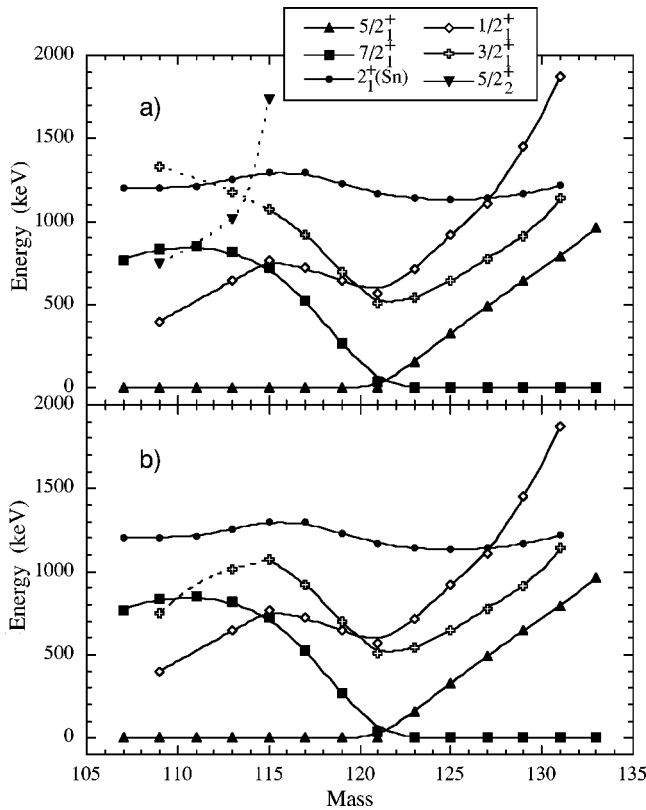


FIG. 9. Systematics of the light Sb isotopes. Energies are shown in units of keV as a function of mass. In (a), the 1018-keV level in  $^{113}\text{Sb}$  and 752-keV level in  $^{109}\text{Sb}$  are shown with  $5/2^+$  spin and parity, while the unassigned 1181-keV level in  $^{113}\text{Sb}$  is assumed to have  $J^\pi=3/2^+$ . The  $3/2^+$  level may increase for lower neutron numbers, suggesting that the new 1331-keV level in  $^{109}\text{Sb}$  may also have  $J^\pi=3/2^+$ . In (b), the 1018-keV level in  $^{113}\text{Sb}$  and 752-keV level in  $^{109}\text{Sb}$  are shown with  $3/2^+$  spin and parity. The  $3/2^+_1$  level is seen to peak at  $N=64$  and decrease for lower neutron numbers, similar to the  $1/2^+_1$  states.

while the ground state transition is quite strong. Little or no beta feeding occurs for the new level at 402 keV. While the 402-keV transition is of moderate intensity, 50% of this intensity may be accounted for by feeding from the suggested levels at 1592 and 1837 keV. In addition, many unplaced coincident transitions shown in Fig. 4 may account for the remaining intensity.

The beta decay of  $^{113}\text{Te}$  has been studied, but may not make a good comparison for  $^{109}\text{Te}$ . The ground state of  $^{113}\text{Te}$  has been proposed to be  $7/2^+$  [13]. The  $5/2^+$  ground state of  $^{113}\text{Sb}$  is fed most strongly in the beta decay, followed by the  $7/2^+_1$  at 814 keV and  $5/2^-_2$  at 1818 keV. In addition, the  $1/2^+$  state at 645 keV and the  $9/2^+_1$  state at 1257 keV appear to be fed with nearly equal intensity. It is unusual to observe  $7/2^+ \rightarrow 1/2^+$  beta decays with such an intensity. A beta-decaying  $1/2^+$  state has been observed at very low energy in  $^{115}\text{Te}$ ; a similar isomeric beta feeding may be occurring in  $^{113}\text{Te}$ . The beta branch to the  $5/2^+$  ground state from the  $7/2^+$  parent is very strong in  $^{113}\text{Te} \rightarrow ^{113}\text{Sb}$ . In  $^{115}\text{Sb}$ , this decay branch is much weaker despite the similar parent ( $7/2^+$ ) and daughter ( $5/2^+$ ) ground state spins.

The beta decay of  $^{115}\text{Te}$  has been studied in greater detail. The known  $7/2^+$  ground state most heavily feeds two  $9/2^+$  states at 1327 and 1381 keV in  $^{115}\text{Sb}$ . By comparison, beta feeding to the known  $9/2^+$  level at 1101 keV in  $^{109}\text{Sb}$  appears very weak, while the level at 752 keV is three times stronger. It is unlikely that the new level at 752 keV has  $9/2^+$  spin and parity as it has not been seen previously in high-spin studies. Therefore, it is unlikely that  $^{109}\text{Te}$  has a  $J \geq 7/2^+$  ground state.

The  $1/2^+$  isomeric state in  $^{115}\text{Te}$  also beta decays, primarily feeding the  $1/2^+$  level at 770 keV in the daughter  $^{115}\text{Sb}$ . As the known  $7/2^+$  state at 832 keV appears to be fed in the  $^{109}\text{Te}$  beta decay, it is unlikely that the  $^{109}\text{Te}$  ground state has  $J \leq 3/2$ .

The ground state of  $^{109}\text{Te}$  is therefore suggested to have  $J^\pi=5/2^+$ , in agreement with expectations. The beta decay of this nuclide is a case of what Kisslinger and Sorenson describe as “even jumping” [14], in which an even number of protons (most likely  $d^2_{5/2}$  for  $^{109}\text{Te}$ ) and an odd neutron (again most likely  $d_{5/2}$  for  $^{109}\text{Te}$ ) undergo either positron or electron capture decay.

Beta decay will transform one member of the  $^{109}\text{Te}$  proton pair into a new neutron, leaving an odd proton. This process will directly populate the ground state of  $^{109}\text{Sb}$  when the  $d_{5/2}$  proton forms a  $d_{5/2}$  neutron via Gamow-Teller decay. The newly formed  $d_{5/2}$  neutron will pair with the odd  $d_{5/2}$  neutron of  $^{109}\text{Te}$  in the daughter  $^{109}\text{Sb}$ . These decays will also strongly populate the  $3/2^+$  state of  $\pi d_{5/2}$  weakly coupled to the  $2^+_1$  of the  $^{108}\text{Sn}$  core.

The  $d_{5/2}$  proton may also undergo spin-flip Gamow-Teller decay to form a  $d_{3/2}$  neutron. A three-quasiparticle level will result, having a configuration involving the initial  $d_{5/2}$  neutron, the new  $d_{3/2}$  neutron, and remaining  $d_{5/2}$  proton. Due to the broken neutron pair and promotion of one neutron from the  $d_{5/2}$  to the  $d_{3/2}$  orbital, these levels may lie near a 4-MeV excitation energy. These “doorway” beta-decay states will be strongly mixed with many other nearby levels.

The experimental data are consistent with this picture. Most of the transitions coincident with the 402-, 752-, and 832-keV levels arise from states 1.5–2.1 MeV in excitation energy. These levels may be fed from high-lying excited states not observed in this experiment.

The high intensity of beta feeding to the proposed new level at 752 keV suggests a  $3/2^+$  or  $5/2^+$  spin and parity. The  $^{109}\text{Sb}$  shell model calculations would favor a  $3/2^+$  assignment, as both calculations suggest relatively low excitation energy for this state. A large amount of beta feeding would also be expected for a  $J^\pi=3/2^+$  state at low energy.

However, comparisons with experimental levels of the heavier Sb isotopes would favor a  $5/2^+_2$  assignment. The  $3/2^+$  state is known in  $^{115}\text{Sb}$  and may be the unassigned state at 1181 keV in  $^{113}\text{Sb}$ . This state appears to increase with lower neutron numbers. A startling change would be needed to bring this state down to 752 keV with the loss of only four neutrons.

Interacting boson-fermion model (IBFM) calculations for  $^{115}\text{Sb}$  [15] suggest that the  $5/2^+_2$  state is not the  $d_{5/2} \otimes 2^+$ , but rather the  $g_{7/2} \otimes 2^+$  or  $d_{5/2} \otimes 0^+_2$ . This implies that the  $d_{5/2}$

$\otimes 2^+$  state has not yet been observed in this nuclide, suggesting that a trend to the lower isotopes is misleading. The  $5/2_2^+$  states have not been confirmed for the odd- $A$  isotopes with  $A \geq 117$ .

If the 1018-keV level in  $^{113}\text{Sb}$  has  $3/2^+$  spin and parity, this would suggest that the  $3/2^+$  state decreases in excitation energy relative to the  $5/2^+$  ground state below  $N=64$  similar to the first  $1/2^+$  level. The absence of a 348-keV transition from the known  $9/2^+$  state at 1101 keV in coincidence with the 752-keV decay supports a  $3/2^+$  assignment.

Therefore, a tentative spin assignment of  $(3/2^+, 5/2^+)$  is suggested for the 752-keV level in  $^{109}\text{Sb}$ , while  $3/2^+$  may be more likely. Experimental energy systematics of the light Sb isotopes ( $N \leq 82$ ) are shown in Fig. 9. The top portion of the figure shows expected trends assuming a  $5/2^+$  spin and parity for the 1018-keV level in  $^{113}\text{Sb}$ . The bottom portion assumes  $3/2^+$  spin and parity for this state.

From systematic trends of low-spin energy levels for Sb isotopes, the 402-keV state of  $^{109}\text{Sb}$  may have  $1/2^+$  spin and parity. This assignment agrees with the absence of apparent beta feeding, as a  $5/2^+ \rightarrow 1/2^+$  beta decay is not expected. In addition, a possible very weak 350-keV coincidence (see Fig. 4) may be due to feeding from the new 752-keV level with  $(3/2^+, 5/2^+)$  spin and parity. A 430-keV decay from the known  $7/2^+$  level at 832 keV is not observed. This further supports a  $J^\pi = 1/2^+$  spin assignment.

Shell model calculations shown in Fig. 8 are also in good agreement for a  $1/2^+$  assignment for the new level at 402 keV. Both calculations suggest a low-energy  $1/2^+$  first excited state for  $^{109}\text{Sb}$ .

## VI. CONCLUSIONS

Low-spin levels in  $^{109}\text{Sb}$  are reported for the first time following population by beta decay. Below 1 MeV, the known  $\pi g_{7/2}$  level at 832 keV was observed with two new levels at 752 and 402 keV. A  $(3/2^+, 5/2^+)$  assignment is suggested for the 752-keV level, and  $(1/2^+)$  for the 402-keV level. Similar to the heavier Sb isotopes, these levels are assumed to arise from weak coupling between the valence proton and  $2_1^+$  of the even-even  $^{108}\text{Sn}$  core. Additional experimental information for low-spin states in  $^{109}\text{Sb}$  and neighboring nuclides is necessary to provide further insight into these structures.

## ACKNOWLEDGMENTS

Support for this work was provided by the U.S. Department of Energy under Contract Nos. DE-FG02-91ER-40609, DE-FGD2-94-ER49834, W-31-109-ENG-38, and DE-AC05-00OR22725.

- 
- [1] R. E. Shroy, A. K. Gaigalas, G. Schatz, and D. B. Fossan, *Phys. Rev. C* **19**, 1324 (1979).
- [2] V. P. Janzen *et al.*, *Phys. Rev. Lett.* **70**, 1065 (1993).
- [3] M. Conjeaud, S. Harar, and Y. Cassagnou, *Nucl. Phys.* **A117**, 449 (1968).
- [4] R. Kammermans, T. J. Ketel, and H. Verheul, *Z. Phys. A* **279**, 99 (1976).
- [5] R. Kirchner *et al.*, *Phys. Lett.* **70B**, 150 (1977).
- [6] J. Blachot, *Nucl. Data Sheets* **86**, 505 (1999).
- [7] H. Schnare *et al.*, *Phys. Rev. C* **54**, 1598 (1996).
- [8] R. Machleidt, F. Sammarruca, and Y. Song, *Phys. Rev. C* **53**, R1483 (1996).
- [9] M. Hjorth-Jensen, T. T. S. Kuo, and E. Osnes, *Phys. Rep.* **261**, 125 (1995).
- [10] R. R. Whitehead, A. Watt, B. J. Cole, and I. Morrison, *Adv. Nucl. Phys.* **9**, 123 (1977).
- [11] E. Dikmen, A. Novoselsky, and M. Vallieres, *Phys. Rev. C* **64**, 067305 (2001).
- [12] E. Dikmen (private communication).
- [13] M. E. J. Wigmans, R. J. Hetnis, P. M. A. van der Kam, and H. Verheul, *Phys. Rev. C* **14**, 243 (1976).
- [14] L. S. Kisslinger and R. Z. Sorenson, *Rev. Mod. Phys.* **35**, 853 (1963).
- [15] Yu. N. Lobach and D. Bucurescu, *Phys. Rev. C* **57**, 2880 (1998).